Structural Evolution of Anionic Silicon Clusters Si_N ($20 \leq N \leq 45$)

Jaeil Bai,[†] Li-Feng Cui,[‡] Jinlan Wang,[§] Soohaeng Yoo,[†] Xi Li,[‡] Julius Jellinek,*[,§] Christof Koehler,[||] Thomas Frauenheim,[||] Lai-Sheng Wang,*[,‡] and Xiao Cheng Zeng*[,†]

Department of Chemistry and Center for Materials Research & Analysis, University of Nebraska, Lincoln, Nebraska 68588, Department of Physics, Washington State University, 2710 University Drive, Richland, Washington 99352, Chemical Sciences Division, Pacific Northwest National Laboratory, P.O. Box 999, MS K8−88, Richland, Washington 99352, Chemistry Division, Argonne National Laboratory, Argonne, Illinois 60439, and Theoretische Physik, Universität-GH Paderborn, D-33098 Paderborn, Germany

Received: October 14, 2005

Results of a combined photoelectron spectroscopy and first-principles density-functional study of Si_N^- clusters in the size range $20 \leq N \leq 45$ are reported and discussed. Evidence for a prolate-to-near-spherical shape transition at $N = 27$ is presented. It is shown that the tricapped-trigonal-prism (TTP) structural motif Si_9 found in most low-lying clusters Si_N^-, $9 \leq N \leq 19$, is replaced or augmented by a series of structural motifs consisting of a bulklike "adamantane" fragment plus a magic-number cluster (Si_6, Si_7, Si_{10}) or TTP Si_9 in low-lying prolate clusters Si_N^-, $N \geq 20$. For $28 \leq N \leq 45$, almost all low-lying near-spherical clusters Si_N^- adopt "stuffed-cage"-like structures where the cages are homologous to carbon fullerenes in the sense that they are composed of only five- and six-membered rings. However the arrangement of the "stuffing" atoms is not yet diamondlike.

Introduction

Silicon plays a vital role in the microelectronic industry. As miniaturization of electronic devices is approaching the nanoscale, it is important to understand the electronic and structural properties of Si_N nanoclusters. The size range that received most attention is $10 < N < 10^2$.[1−28] Experimentally, the structures of very small silicon clusters ($N < 8$) have been inferred from molecular spectroscopy[3] and high-resolution photoelectron spectroscopy (PES)[28] measurements. For larger Si clusters, structural shape information has been obtained on basis of ion mobility data by Jarrold and co-workers.[19,20] It has been found that medium-sized low-lying clusters are mostly prolate in shape for $N < 27$ and become near spherical for $N > 27$. A computational study based on a genetic algorithm search procedure[13] uncovered a generic structural feature in low-lying neutral clusters Si_N, $N = 10−18$, that is, nearly all clusters contain the tricapped-trigonal-prism (TTP) Si_9 motif. The most compelling evidence was later provided by Müller et al.[11] who both measured and simulated anion PES spectra in the size range $8 \leq N \leq 20$ and validated the presence of the TTP structural motif in many medium-sized low-lying Si_N^- clusters. Indeed, the combined experimental and theoretical PES approach has become a very effective method to identify cluster structures.[10,11,29−31]

However, the combined theoretical/experimental approach is most effective when the following two conditions are met: (1) Well-resolved PES spectra can be obtained, particularly for the first two or three PES peaks near the threshold as they are directly related to the frontier orbitals of the cluster (because of congested electronic transitions, multiple low-energy isomers, or high cluster temperatures, well-resolved PES spectra are rather difficult to measure). (2) A large database on low-energy clusters is available, typically obtained via using various global optimization techniques, e.g., genetic algorithms,[13] basin-hopping method,[32a] or minima-hopping method,[32b] combined with first-principles calculations.[33−35] We have obtained well-resolved PES spectra for Si_N^- ($N = 5−50$) at several photon energies by controlling cluster temperatures from a laser vaporization supersonic cluster source. On the other hand, in our density functional theory (DFT) calculations, many candidate structures (or database of low-lying clusters) have been reported in the literature.[14−18] On the basis of the calculated electron binding energies along with the measured PES spectra, we are able to identify some new generic structural features in low-lying prolate-shaped Si_N^- clusters and to provide spectroscopic corroboration of the prolate-to-spherical shape transition at $N = 27$.

Methods

Experimental. The experiments were carried out using a magnetic bottle time-of-flight photoelectron spectrometer, details of which have been described previously.[36] The Si_N^- cluster anions were produced by laser vaporization of a pure silicon target with a helium carrier gas and analyzed using a time-of-flight mass spectrometer. The Si_N^- ($N = 5−50$) species were mass selected and decelerated before crossing with a detachment laser beam (266, 193, and 157 nm) in the interaction zone of the magnetic-bottle photoelectron analyzer. Well-resolved photoelectron spectra for cold Si_N^- clusters (Supporting Information) were obtained by carefully selecting those clusters that had sufficient resident time in the nozzle to be thermalized (within a temperature range of 300−500 K).[37,38] Photoelectrons were collected at nearly 100% efficiency by the magnetic bottle and analyzed in a 3.5-m-long electron flight tube. The binding energy spectra were obtained by subtracting the kinetic energy spectra from the photon energies of the detachment laser. The spectra

* To whom correspondence should be addressed. E-mail: ls.wang@pnl.gov (L.S.W.); xczeng@phase2.unl.edu (X.C.Z.); Jellinek@anl.gov (J.J.).
[†] University of Nebraska.
[‡] Washington State University.
[§] Argonne National Laboratory.
[||] Universität-GH Paderborn.

10.1021/jp055874s CCC: $33.50
Published on Web 12/16/2005

TABLE 1: Calculated Total Energy Differences (eV) with Respect to the Isomer with the Lowest Energy for Si_{20}^-−Si_{29}^- Shown in Figures 1 and 2

anion	energy difference (primary isomer)	energy difference (secondary isomer)	energy difference (tertiary isomer)
Si_{20}^-	0.0	0.011	
Si_{21}^-	0.0	0.303	
Si_{22}^-	0.0	0.411	
Si_{23}^-	0.0	0.326	
Si_{24}^-	0.0	1.004	
Si_{25}^-	0.0	0.022	
Si_{26}^-	0.008	0.0	
Si_{27}^-	0.0	0.104	0.252
Si_{28}^-	0.127	0.0	0.093
Si_{29}^-	0.279	0.0	0.301

were calibrated using the known spectrum of Au^-. The apparatus has an electron energy resolution of $\Delta E/E \approx 2.5\%$, i.e., about 25 meV for 1 eV electrons.

Theoretical. Details of the theoretical methodology and searches for candidate structures of low-lying silicon clusters have been published elsewhere.[17,18,27] The searches generated a large database for low-energy neutral and anion clusters. For prolate-shaped clusters (in the size range of $12 \le N \le 30$), we adopted the basin-hopping (BH) method[32] combined with DFT.[33] In the DFT-BH search,[18] the Monte Carlo scheme is used to explore the potential-energy surface. The potential energy and energy gradient-driven optimizations were computed by using the CPMD code.[33] For larger near-spherical clusters (in the size range $25 \le N \le 45$), we took a two-step approach.[17] The first step is a global search of the potential-energy surface by using a genetic algorithm[13] coupled with the tight-binding model.[25] The second step is an augmented search using the DFT-BH method or the minima-hopping method coupled with the density-functional tight-binding (DFTB) theory,[34] based on those low-energy structures obtained in the first step. For all clusters, after the low-energy anion isomers were identified, all-electron DFT optimizations at the PBEPBE/6-31G(d) level of theory and basis set, as implemented in the Gaussian 03 code,[35] were performed. Total energies of low-lying anion clusters are listed in Table S1 (Supporting Information) and the total energy differences with respect to the lowest-energy anion isomers (for $20 \le N \le 29$) are listed in the Table 1. Finally, simulated PES spectra of low-energy isomers were obtained from the negatives of the Kohn−Sham (KS) eigenenergies by shifting them so that the negative of the highest-occupied molecular orbital (HOMO) KS eigenenergy coincides with the computed value of the vertical detachment energy (VDE). The one or two cases that provide the best fit to the measured PES spectra are shown in Figures 1−3.

Results and Discussion

The PES of Si_N^- ($N = 20-26$) measured at 193 nm are shown in column a of Figure 1, where X and A (peaks) mark the first two electronic levels of the *primary* isomer and X′ and A′ denote the first two electronic levels of a *secondary* isomer. Here the "primary isomer" refers to the isomer that gives rise to the most conspicuous peaks in the PES. Some weak features in the spectra, however, are presumably due to one or a few secondary isomers. The spectra are consistent with the results of a previous PES study[9] that had a somewhat lower resolution. For Si_N^- ($N = 20-26$), we observed fairly large gaps between the binding energies of the two most external electrons (0.5−1.0 eV) for the *primary* anion isomers, implying that the corresponding neutral Si_N clusters are all closed-shell systems with a reasonably large HOMO−lowest-unoccupied molecular orbital (LUMO) gap. Among these clusters, Si_{25}^- exhibited the largest gap (1.0 eV), which is already quite close to that of bulk silicon (1.12 eV). The VDEs of both the primary and secondary isomers are listed in Table 2.

TABLE 2: Measured and Computed VDEs of Primary and Secondary Isomers of Si_{20}^-−Si_{26}^- Shown in Figures 1 and 2

anions		VDE (eV) experimental	VDE (eV) theoretical
Si_{20}^-	X	3.57	3.587
	X′	3.38	3.491
Si_{21}^-	X	3.57	3.564
	X′	3.16	3.031
Si_{22}^-	X	3.37	3.299
	X′	3.23	3.155
Si_{23}^-	X	3.26	3.194
	X′	3.12	3.124
Si_{24}^-	X	3.66	3.597
	X′	3.34	3.336
Si_{25}^-	X	3.21	3.206
	X′	3.60	3.571
Si_{26}^-	X	3.34	3.311
	X′	3.02	3.153

In columns b and c of Figure 1, we plot the simulated PES spectra of the primary and the most plausible secondary isomer. As is shown from the figure, the simulated spectra of the primary isomers are in very good agreement with the experimental PES data. The computed spectra for the leading secondary isomers can account for many weak PES features. We found that the primary isomers of Si_{20}^-−Si_{26}^- and the leading secondary isomers of Si_{20}^-−Si_{25}^- are all prolate in shape. Moreover, these clusters contain a bulklike fragment, either a six-atom (the puckered hexagonal ring highlighted in green color) or a nine-atom (two fused hexagonal rings highlighted in pink color) subunit of the "adamantane" Si_{10} (Figure 4).[1,21,22] Note that the six-atom subunit has been identified earlier in smaller anion clusters (Si_{16}^- and Si_{17}^-)[11] as well as in neutral clusters ($Si_{16} - Si_{20}$),[18] and these two subunits are always coupled with one or two magic-number cluster (Si_6, Si_7, Si_{10})[4,15,16,18] or the TTP Si_9. It should be noted that the leading secondary isomer of Si_{26}^- is no longer prolate in shape, and it is more compact and near spherical.

A dramatic spectral change is observed at Si_{27}^- (Figure 2a), whose PES spectrum is featureless while the spectra for many clusters larger than Si_{27}^- again exhibit resolvable features up to Si_{45}^- (Figures 2 and 3). This observation suggests that there must be *several coexisting* isomers for Si_{27}^- and many clusters larger than Si_{27}^-, which contribute to the spectrum more or less equally. In other words the prolate isomer does not dominate any more. This observation is in complete agreement with the ion mobility experiments by Jarrold and co-workers,[19,20] who found a structural transition from prolate to near-spherical shapes for Si_N^- clusters in the size range $N = 27-29$. Our study shows that indeed for $N < 26$ both the primary and the leading secondary isomer of Si_N^- are of prolate shape (Figure 1), whereas for Si_{26}^- the primary isomer is prolate, but the leading secondary isomer is near spherical. It is natural then that for Si_{27}^- the prolate and some near-spherical isomers *coexist* and that, for clusters larger than $N = 27$, the near-spherical isomers are expected to become more and more competitive energetically than the prolate isomers (Table 1).

Two questions arise: (1) What are the structures of the near-spherical clusters? (2) Are there any generic structural features in these near-spherical clusters? Numerous candidates for the near-spherical clusters have been reported recently[17] for $N > 26$. In Figure 2, we compare experimental PES for Si_{27}^-−Si_{29}^-

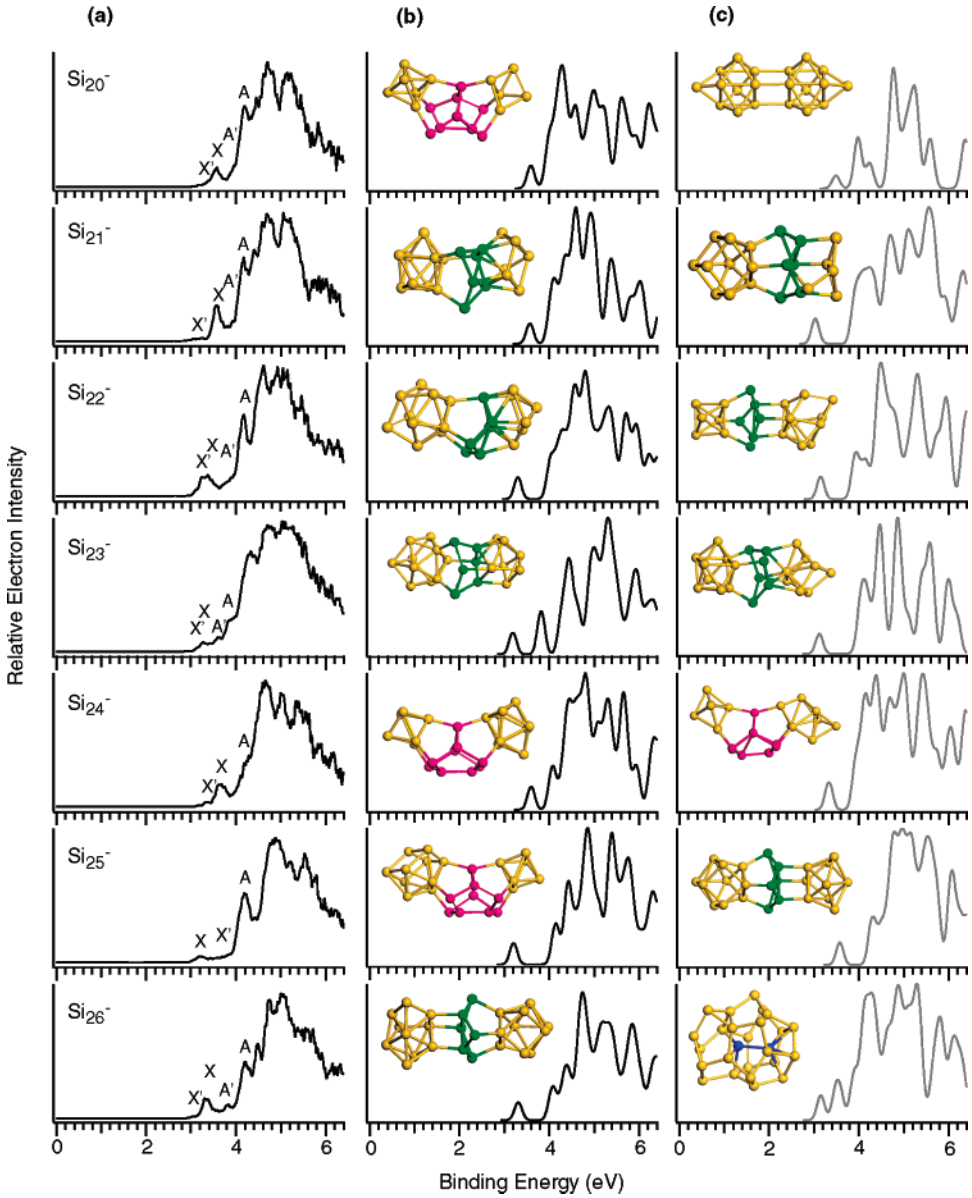

Figure 1. Comparison of measured and simulated PES spectra for Si_{20}^{-}−Si_{26}^{-}. (a) Spectra measured at 193 nm (6.424 eV). X and A (X′ and A′) denote the first and second photoelectron peaks for the primary (secondary) isomers. (b) Simulated spectra for the primary isomers. (c) Simulated spectra for the secondary isomers. The simulated spectra were obtained by convoluting the discrete DFT energy eigenvalues with Gaussians of width 0.08 eV. The primary isomer provides the best comparison with the measured spectra (e.g., the location of the threshold peak X as well as the separation between the first and the second major peak A). The secondary isomer is intended to compare with certain weak features in the spectra (e.g., the X′ and A′ peaks).

to simulated spectra with three low-energy isomers: two near-spherical (panels b and c) and one prolate (panel d). Each of the three simulated spectra of Si_{27}^{-} is highly structured. The measured spectrum of this cluster however is largely featureless. This suggests that all these three isomers of Si_{27}^{-} contribute about equally to the measured spectrum. The same can be said about Si_{28}^{-}. However, for Si_{29}^{-} only the simulated spectra of the primary and one secondary isomer (panel b) appear to agree with the measured spectrum (panel a), suggesting that the prolate isomer of Si_{29}^{-} (panel d) has a negligible contribution.

In Figure 3, we compare the experimental PES with the simulated spectra for the leading candidate of the lowest-energy isomer of Si_N^{-}, $N = 30-45$. For most sizes, there are certain degrees of agreement between the experiment and the computations, for example, the location of the first peak and for some clusters, even the location of the second peak. For Si_{30}^{-}, we computed PES of a prolate isomer that has the lowest energy in our database, and we found that the simulated PES entails a large energy gap between the first and second peak (like Figure 2d for Si_{29}^{-}). We therefore conclude that the low-lying isomers of Si_{30}^{-}−Si_{45}^{-} are most likely near spherical in shape and exhibit "stuffed-cage"-like structures. Interestingly, theoretical calculations indicate that the cages of these candidate low-lying isomers are all homologous to the carbon fullerene cages in the sense that they are composed of only pentagonal and hexagonal rings and have even numbers of Si atoms. In Figures 2 and 3, we highlight the core-filling ("stuffing") atoms inside the cages with blue color. If these core-filling atoms were removed and the cage atoms were replaced by carbon atoms, one would obtain the fullerene cages after structural relaxation.[17] The reasonable match between the measured and simulated PES spectra provides additional spectroscopic support to the view that the near-spherical low-lying silicon clusters all exhibit a "stuffed-fullerene"-like structural feature. In Figure 5, we display two low-energy isomers of Si_{45} obtained in two different studies.[17,27] One can see that both isomers have "stuffed-

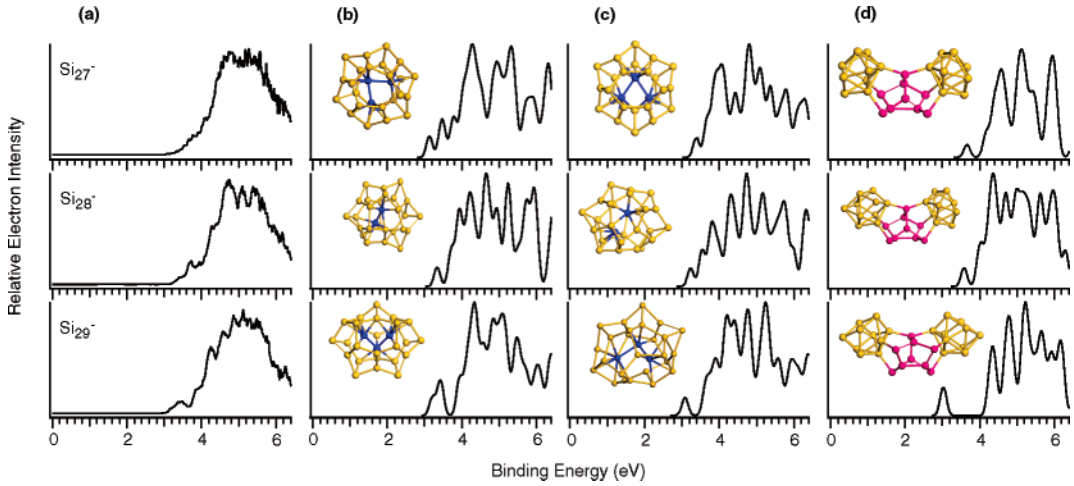

Figure 2. The same as Figure 1 but for $Si_{27}^- - Si_{29}^-$.

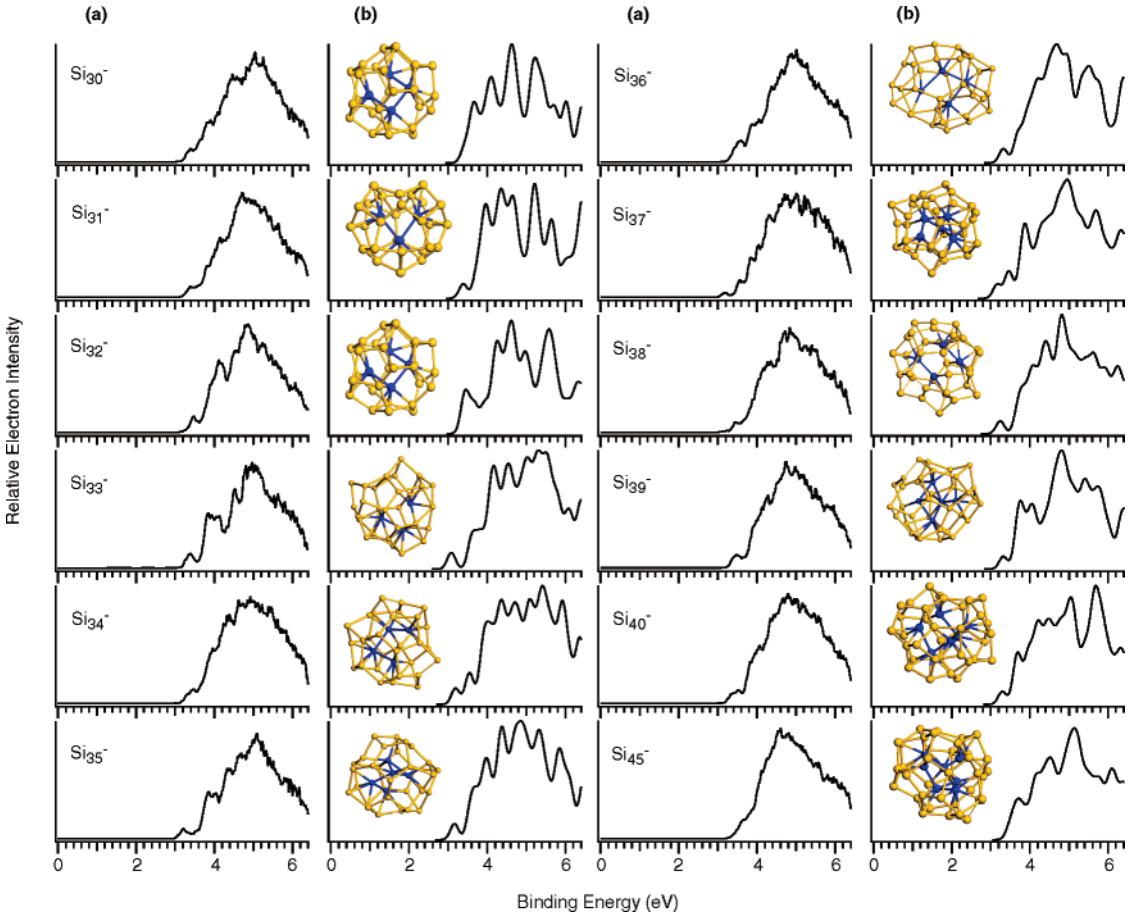

Figure 3. The same as Figure 1 but for $Si_{30}^- - Si_{40}^-$ and Si_{45}^-.

fullerene"-like structures with seven core-filling atoms. The core-filling subunits however do not exhibit diamondlike tetrahedral packing characteristic of bulk silicon with diamond structure.

Summary

Our joint experimental and theoretical study confirms that anionic silicon clusters undergo a major structural change at $N = 27$. The well-resolved PES spectra in the size range of $20 \leq N \leq 26$ allow us to identify some generic structural features for the low-lying prolate clusters. On the basis of these

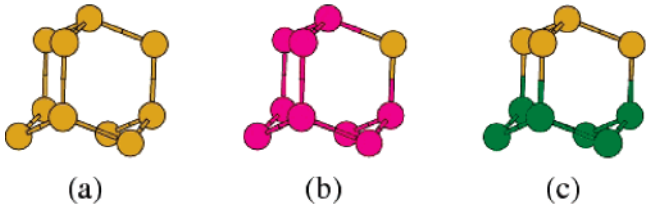

Figure 4. (a) A bulk fragment of the cubic diamond silicon, "adamantane" Si_{10}. (b) A nine-atom subunit of the Si_{10}, two fused puckered hexagonal rings, highlighted in pink color. (c) A six-atom subunit of the Si_{10}, a puckered hexagonal ring, highlighted in green color.

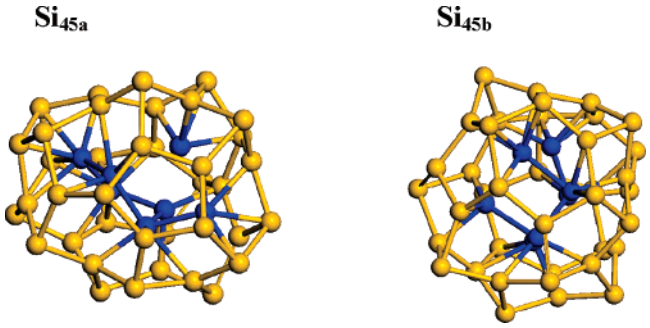

Figure 5. Two low-energy Si_{45} isomers obtained respectively from two potential-energy-surface searches (refs 27 and 17). The Si_{45a} isomer has the lowest energy. The endohedral core-filling Si atoms are highlighted in blue color.

structures, new structural motifs are identified for silicon clusters in this size range, complement to the well-known TTP Si_9 structural motif for $N \leq 20$. These new motifs contain a diamondlike fragment, either a six-atom or a nine-atom subunit of the "adamantane" Si_{10}, coupled with one or two magic-number clusters (Si_6, Si_7, Si_{10})[4,5,15,16,18] or the TTP Si_9. To some extent, the present study also offers spectroscopic support to an earlier suggested notion[21−26,17] that the carbon fullerene cages can be a generic cage motif for building near-spherical low-energy silicon clusters in the size range $26 \leq N \leq 45$.

Acknowledgment. We thank Professor K. A. Jackson, Professor B. C. Pan, Dr. M. R. Pederson, Dr. J. J. Zhao, and Dr. Jun Li for valuable discussions. The experimental work done at Washington State was supported by the National Science Foundation (DMR-0503383) and performed at the EMSL, a national scientific user facility sponsored by the DOE's Office of Biological and Environmental Research and located at the Pacific Northwest National Laboratory, operated for DOE by Battelle. The theoretical work done at Nebraska was supported by grants from the DOE's Office of Basic Energy Sciences (DE-FG02-04ER46164), National Science Foundation (CHE, DMII and MRSEC), the John Simon Guggenheim Foundation, the Nebraska Research Initiative, and the University of Nebraska—Lincoln Research Computing Facility. The theoretical work at Argonne was supported by DOE's Office of Basic Energy Sciences, Division of Chemical Sciences, Geosciences, and Biosciences, under Contract No. W-31-109-Eng-38.

Supporting Information Available: Complete ref 35, calculated total energies, and measured PES. This material is available free of charge via the Internet at http://pubs.acs.org.

References and Notes

(1) Jarrold, M. F. *Science* **1991**, *252*, 1085−1092.
(2) Brown, W. L. *Science* **1987**, *235*, 860−865.
(3) Honea, E. C.; Ogura, A.; Murray, C. A.; Raghavachari, K.; Sprenger, W. O.; Jarrold, M. F.; Brown, W. L. *Nature* **1993**, *366*, 42−45.
(4) Zhang, Q. L.; Liu, Y.; Curl, R. F.; Tittel, F. K.; Smalley, R. E. *J. Chem. Phys.* **1998**, *88*, 1670−1677.
(5) Raghavachari, K.; Rohlfing, C. M. *J. Chem. Phys.* **1988**, *89*, 2219−2234.
(6) Jarrold, M. F.; Honea, E. C. *J. Phys. Chem.* **1991**, *95*, 9181−9185.
(7) Marsen, B.; Lonfat, M.; Scheier, P.; Sattler, K. *Phys. Rev. B* **2000**, *62*, 6892−6895.
(8) Maus, M.; Gäntefor, G.; Eberhardt, W. *Appl. Phys. A.* **2000**, *70*, 535−539.
(9) Hoffmann, M. A.; Wrigge, G.; Issendorff, B. v.; Müller, J.; Ganteför, G.; Haberland, H. *Eur. Phys. J. D* **2001**, *16*, 9−11.
(10) (a) Binggeli, N.; Martins, J. L.; Chelikowsky, J. R. *Phys. Rev. Lett.* **1992**, *68*, 2956−2959. (b) Binggeli, N.; Chelikowsky, J. R. *Phys. Rev. Lett.* **1995**, *75*, 493−496. (c) Ogut, S.; Chelikowsky, J. R.; Louie, S. G. *Phys. Rev. Lett.* **1997**, *79*, 1770−1773.
(11) Müller, J.; Liu, B.; Shvartsburg, A. A.; Ogut, S.; Chelikowsky, J. R.; Siu, K. W. M.; Ho, K.-M.; Gantefor, G. *Phys. Rev. Lett.* **2000**, *85*, 1666−1669.
(12) Giovanni, M.; Ferguson, M. J.; Sheehan, S. M.; Neumark, D. M. *Chem. Phys. Lett.* **2004**, *399*, 389−391.
(13) Ho, K.-M.; Shvartsburg, A. A.; Pan, B.; Lu, Z.-Y.; Wang, C.-Z.; Wacker, J. G.; Fye, J. L.; Jarrold, M. F. *Nature* **1998**, *392*, 582−585.
(14) Mitas, L.; Grossman, J. C.; Stich, I.; Tobik, J. *Phys. Rev. Lett.* **2000**, *84*, 1479−1482.
(15) Rata, I.; Shvartsburg, A. A.; Horoi, M.; Frauenheim, T.; Siu, M. W. M.; Jackson, K. A. *Phys. Rev. Lett.* **2000**, *85*, 546−549.
(16) Jackson, K. A.; Horoi, M.; Chaudhuri, I.; Frauenheim, T.; Shvartsburg, A. A. *Phys. Rev. Lett.* **2004**, *93*, 013401−1−4.
(17) (a) Yoo, S.; Zhao, J. J.; Wang, J.; Zeng, X. C. *J. Am. Chem. Soc.* **2004**, *126*, 13845−13849. (b) Zhao, J.; Wang, J.; Jellinek, J.; Yoo, S.; Zeng, X. C. *Eur. Phys. J. D* **2005**, *34*, 35−37. (c) Wang, J.; Zhou, X.; Wang, G.; Zhao, J. *Phys. Rev. B.* **2005**, *71*, 1134121−1134124.
(18) Yoo, S.; Zeng, X. C. *Angew. Chem., Int. Ed.* **2005**, *44*, 1491−1495.
(19) Jarrold, M. F.; Constant, V. A. *Phys. Rev. Lett.* **1991**, *67*, 2994−2997.
(20) Hudgins, R. R.; Imai, M.; Jarrold, M. F.; Dugourd, P. *J. Chem. Phys.* **1999**, *111*, 7865−7870.
(21) Tomanek, D.; Schluter, M. A. *Phys. Rev. Lett.* **1986**, *56*, 1055−1058.
(22) Kaxiras, E. *Phys. Rev. Lett.* **1990**, *64*, 551−554.
(23) Jelski, D. A.; Swift, B. L.; Rantala, T. T.; Xia, X.; George, T. F. *J. Chem. Phys.* **1991**, *95*, 8552−8560.
(24) Röthlisberger, U.; Andreoni, W.; Parrinello, M. *Phys. Rev. Lett.* **1994**, *72*, 665−668.
(25) Menon, M.; Subbaswamy, K. R. *Phys. Rev. B* **1995**, *51*, 17952−17956.
(26) Sun, Q.; Wang, Q.; Jena, P.; Waterman, S.; Kawazoe, Y. *Phys. Rev. A* **2003**, *67*, 063201−1−6.
(27) Yoo, S.; Zeng, X. C.; Zhu, X.; Bai, J. *J. Am. Chem. Soc.* **2003**, *125*, 13318−13319.
(28) Arnold, C. C.; Neumark, D. M. *J. Chem. Phys.* **1993**, *99*, 3353−3362.
(29) Bonacic-Koutecky, V.; Fantucci, P.; Koutecky, J. *J. Chem. Phys.* **1989**, *91*, 3794−3795.
(30) (a) Boldyrev, A. I.; Wang, L. S. *J. Phys. Chem. A* **2001**, *105*, 10759−10775. (b) Li, J.; Li, X.; Zhai, H. J.; Wang, L. S. *Science* **2003**, *299*, 864−867.
(31) (a) Acioli, P. H.; Jellinek, J. *Phys. Rev. Lett.* **2002**, *89*, 2134201−2134204. (b) Jellinek, J.; Acioli, P. H. *J. Phys. Chem. A* **2002**, *106*, 10919−10925. (c) Acioli, P.; Jellinek, J. *Eur. Phys. J. D* **2003**, *24*, 27−32. (d) Jellinek, J.; Acioli, P. H. *Metal−Ligand Interactions*; Russo, N., Salahub, D. R., Witko, M., Eds.; Kluwer: Dordrecht, 2003; pp 121−151.
(32) (a) Wales, D. J.; Scheraga, H. A. *Science* **1999**, *285*, 1368−1372. (b) Goedecker, S. *J. Chem. Phys.* **2004**, *120*, 9911−9917.
(33) Hutter, J.; Alavi, A.; Deutsch, T.; Bernasconi, M.; Goedecker, S.; Marx, D.; Tuckerman, M.; Parrinello, M. *CPMD*; Max-Planck-Institue für Festkörperforschung: Stuttgart, 1997−2001; Version 3.9.1.
(34) Porezag, D.; Frauenheim, T.; Köhler, T.; Seifert, G.; Kaschner, R. *Phys. Rev. B* **1995**, *51*, 12947−12957.
(35) Frisch, M. J.; Trucks, G. W.; Schlegel, H. B.; Scuseria, G. E.; Robb, M. A.; Cheeseman, J. R.; J. A. Montgomery, J.; Vreven, T.; Kudin, K. N.; Burant, J. C.; Millam, J. M.; Iyengar, S. S.; Tomasi, J.; Barone, V.; Mennucci, B.; Cossi, M.; Scalmani, G.; Rega, N.; Petersson, G. A.; Nakatsuji, H.; Hada, M.; Ehara, M.; Toyota, K.; Fukuda, R.; Hasegawa, J.; Ishida, M.; Nakajima, T.; Honda, Y.; Kitao, O.; Nakai, H.; Klene, M.; Li, X.; Knox, J. E.; Hratchian, H. P.; Cross, J. B.; Adamo, C.; Jaramillo, J.; Gomperts, R.; Stratmann, R. E.; Yazyev, O.; Austin, A. J.; Cammi, R.; Pomelli, C.; Ochterski, J. W.; Ayala, P. Y.; Morokuma, K.; Voth, G. A.; Salvador, P.; Dannenberg, J. J.; Zakrzewski, V. G.; Dapprich, S.; Daniels, A. D.; Strain, M. C.; Farkas, O.; Malick, D. K.; Rabuck, A. D.; Raghavachari, K.; Foresman, J. B.; Ortiz, J. V.; Cui, Q.; Baboul, A. G.; Clifford, S.; Cioslowski, J.; Stefanov, B. B.; Liu, G.; Liashenko, A.; Piskorz, P.; Komaromi, I.; Martin, R. L.; Fox, D. J.; Keith, T.; Al-Laham, M. A.; Peng, C. Y.; Nanayakkara, A.; Challacombe, M.; Gill, P. M. W.; Johnson, B.; Chen, W.; Wong, M. W.; Gonzalez, C.; Pople, J. A. *Gaussian 03*, Revision C.02; Gaussian, Inc.: Wallingford, CT, 2004.
(36) Wang, L. S.; Wu, H. *Advances in Metal and Semiconductor Clusters. IV. Cluster Materials*; Duncan, M. A., Eds.; JAI: Greenwich, CT, 1998; pp 299−343.
(37) Akola, J.; Manninen, M.; Hakkinen, H.; Landman, U.; Li, X.; Wang, L. S. *Phys. Rev.* B **1999**, *60*, R11297−R11300.
(38) Wang, L. S.; Li, X. *Clusters and Nanostructure Interfaces*; Jena, P., Khanna, S. N., Rao, B. K., Eds.; World Scientific: New Jersey, 2000; pp 293−300.